

## Domain wall motion in micron-sized permalloy elements

R. D. Gomez, T. V. Luu, A. O. Pak, and I. D. Mayergoyz

Laboratory for Physical Sciences, College Park, Maryland 20740 and Department of Electrical Engineering, University of Maryland, College Park, Maryland 20742

K. J. Kirk and J. N. Chapman

Department of Physics and Astronomy, University of Glasgow, Glasgow G12 8QQ, United Kingdom

The magnetization reversal process in an array micron sized NiFe patterns was studied using magnetic force microscopy in the presence of external fields. The behavior of the magnetization distribution was correlated with the aspect ratio and the direction of the applied fields. Magnetizing along the hard axis was found to produce solenoidal magnetization at remanence while applying the field along the easy axis tend to form nonsolenoidal configurations. The micromagnetic evolution, which involved domain wall, crosstie, and vortex displacements, was studied and the correlations were consistent with previously reported  $M-H$  loop observations and theoretical predictions.

© 1999 American Institute of Physics. [S0021-8979(99)21208-X]

Understanding the characteristics of patterned NiFe films at the nanometric length scales is an area of immense scientific and technological importance. Sophisticated numerical micromagnetic modeling combined with advanced fabrication and diagnostic techniques are making it possible to predict and engineer the magnetic properties of submicron sized islands. Smyth *et al.*<sup>1</sup> have investigated the role of particle size, aspect ratio, and interparticle spacing on the hysteretic properties of the ensemble and compared them with *ab initio* calculations while Zhu *et al.*<sup>2</sup> have modeled the micromagnetics of exchanged biased ten micron sized islands and demonstrated remarkable agreement between the model and the measurements. More recently, Schrefl *et al.*<sup>3</sup> have systematically studied the influence of edge shapes on the switching dynamics of submicron particles using Lorentz transmission electron microscopy (LTEM) and micromagnetics to demonstrate how the end shapes affect the switching field. Prior to these, Fredkin *et al.*<sup>4</sup> had developed micromagnetic codes which showed complex edge and multivortex structures depending upon the exact manner in which the magnetic field was applied and the later confirmed by Hefferman *et al.*<sup>5</sup> using Lorentz electron microscopy.

In this article, we augment our knowledge of NiFe islands by building upon these previous works. Specifically, we are interested in characterizing the magnetic evolution of small magnetic elements and in establishing the behavior of domain walls, Bloch lines and crosstie inclusions on these islands by using magnetic force microscopy.

The patterns were prepared by electron beam lithography on silicon-based substrates.<sup>6</sup> The material is an evaporated soft Ni<sub>80</sub>Fe<sub>20</sub> alloy ( $B_s = 1.2$  T), 26 nm thick. The substrate was diced to about 2 mm and was placed inside the gap of an electromagnet. The setup allows magnetic force microscopy images<sup>7</sup> to be acquired while a well controlled continuously variable in-plane magnetic field was applied. Low moment tips were selected to minimize tip-induced perturbations.<sup>8</sup>

To clarify the imaging contrast using MFM in NiFe patterns, the familiar closure pattern of a  $3\ \mu\text{m} \times 3\ \mu\text{m}$  island is shown in Fig. 1 at zero field. Since the MFM detects the divergence of magnetization or the magnetic charge distribution, the contrast comes primarily from the domain boundaries and not from the domain itself. The divergence of the local magnetization at the domain boundary produces the negative and positive charges which appear as dark and bright contrasts along the walls. Based on this, the distribution of charges at all the domain walls and the magnetization of the domains can be qualified. In this case, the four walls along the diagonal are clearly visible and appear to converge into a single point at the center. They divide the element into four triangular domain segments which form the solenoidal closure pattern. Since the magnetization of two adjacent do-

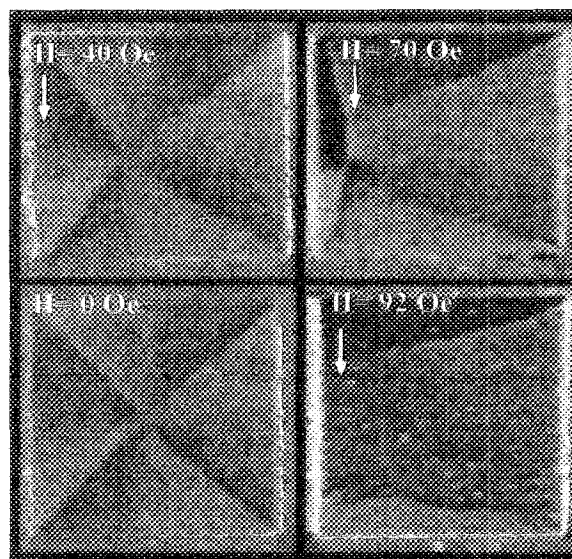


FIG. 1. Evolution of four domain closure pattern of a  $3\ \mu\text{m} \times 3\ \mu\text{m}$  island as a function of applied field. The field was raised monotonically from zero while imaging.

mains are perpendicular to each other, the boundaries are designated as  $90^\circ$  domain walls.

As expected, the application of the field (indicated by the arrows) causes domain wall motion. At 40 Oe the right domain whose magnetization is parallel to the field increases in size at the expense of the left domain. That the central vortex moves horizontally from left to right but remains more or less at the vertical midpoint indicates that there is no preferential growth or shrinkage of the top and bottom domains. However, the subtle enhancement of the contrast at these regions indicates increased nonuniformity of the magnetization distribution inside the domains. By cycling the field within a small field range (under 40 Oe), we established that the magnetization configuration is reversible. However, the system becomes irreversible as soon as the left and right domains meet to form a near- $180^\circ$  domain wall. This is illustrated at  $H=70$  Oe. We note with care that the  $180^\circ$  wall undergoes a contrast reversal at approximately the middle part of the wall which indicates that the newly created  $180^\circ$  wall is comprised of an alternating dipole strip joined by a Bloch line. Bloch lines lower the magnetostatic energy of the wall without introducing large perturbations of the magnetization distributions of the adjoining domains. Hence, in MFM images Bloch lines appear as contrast reversal of  $180^\circ$  walls, with minimal contrast variations in the direction transverse to the wall itself. (This will be later contrasted with the crosstie.) At the next field increment of 92 Oe, the  $180^\circ$  wall has vanished as unfavorable (left) domain has ceded. Comparison of the contrast at  $H=0$  and 92 Oe convincingly shows the redistribution of the magnetic charges on the top and bottom edges of the element as the system evolves from remanence to near saturation. The above process was also seen for similar NiFe islands using high resolution electron microscopy.<sup>9</sup>

Next we consider the behavior of a seven-domain pattern in Fig. 2. This configuration was observed in the same  $3\ \mu\text{m}\times 3\ \mu\text{m}$  element at a different magnetization cycle and is consistent with the observations using transmission electron microscopy (TEM).<sup>9</sup> The schematic diagram of the domain configuration is drawn below to aid in identifying the individual domains. An interesting feature of this pattern is the existence of a crosstie inclusion (at  $H=0$ ) on the rightmost  $180^\circ$  wall which separates the central and right domains. The location of the crosstie on the  $180^\circ$  wall is marked by a closed circle on the diagram. In contrast to a Bloch line, the MFM signature of a crosstie is a contrast reversal that starts at a  $180^\circ$  wall and extends perpendicular to the wall itself and into the adjoining magnetic domains. The magnetization of the left and right domains are pointed in the same direction and both domains expand with increasing field. The image at 62 Oe shows that the middle domain is being overrun by growing domains on both sides. Note that the growth of the left domain is more rapid than the right, which suggests the stabilizing effect of the crosstie inclusion against domain motion. Nevertheless, the Zeeman energy at 70 Oe has become too large that the crosstie itself has collapsed resulting in the coalescence of the expanding domains. Note that the triangular peripheral domains at the bottom have disappeared and reformed into one domain with

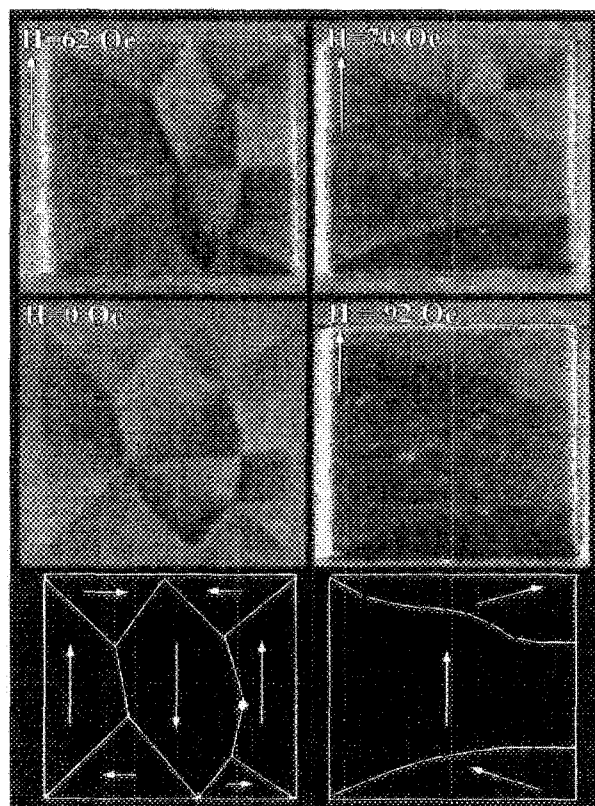


FIG. 2. Evolution of a seven domain closure pattern with crosstie inclusion of  $3\ \mu\text{m}\times 3\ \mu\text{m}$  island as a function of applied field. The inferred pattern is drawn below the images for the zero field (left) and 92 Oe images. The "dot" on the zero field indicates the location of the crosstie inclusion on the near  $180^\circ$  wall.

a curved interior wall. The upper region, on the other hand, still retains traces of the original multidomain structure. This image may falsely suggest that the system exhibits a hybrid configuration, i.e., it is comprised of a multidomain upper structure and a single domain lower structure. We believe that this is not the case here, but the observed anomaly is a manifestation of probe-induced switching. During the first half of the MFM scan, the system was probably in the multidomain configuration akin to that at 62 Oe, but midway into the scan, the slight magnetic field from the probe has induced the switching into the near saturated configuration. The very next image acquired without changing the external field was very similar to the image at 92 Oe, which shows no multidomain structures on top. The near saturation configuration as inferred in the image is shown in the schematic diagram on the right.

The micromagnetic evolution of a slightly different aspect ratio island is shown in Fig. 3. This is a  $2\ \mu\text{m}\times 3\ \mu\text{m}$  rectangular island, which at remanence exhibits a closure configuration with curved walls to compensate for the 1.5 aspect ratio. (The image at  $H=10$  Oe is shown which apart from being cleaner is identical with the image at  $H=0$ .) The behavior at low field is similar to the four domain square in Fig. 1, except that the system is reversible at higher fields (up to about 90 Oe). Irreversible behavior was observed as soon as the coalescence of the left and right domains transpire, occurring at about 105 Oe. It is interesting to note that newly created  $180^\circ$  wall is itself subdivided into three segments

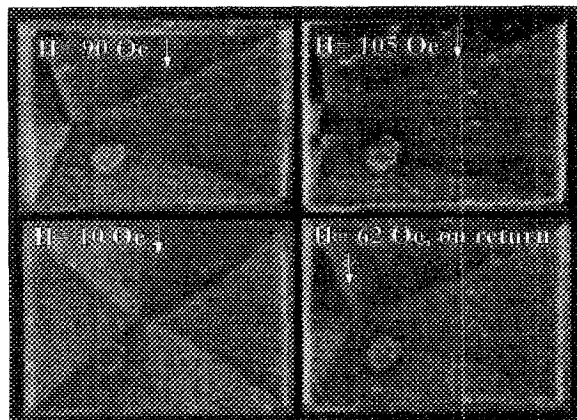


FIG. 3. Evolution of a  $2\ \mu\text{m} \times 3\ \mu\text{m}$ , four domain closure pattern with field along the hard axis showing the emergence and disappearance of a crosstie structure at intermediate fields. (The contaminating precipitate appear to have no influence on the domain wall movement.)

formed by two Bloch lines and a crosstie near the middle. (Comparison of structure with the single Bloch line structure in the  $3\ \mu\text{m}$  square island in Fig. 1 is very helpful in distinguishing crossties and Bloch lines in MFM images.)

We now turn our attention to a  $2\ \mu\text{m} \times 4\ \mu\text{m}$  element shown in Fig. 4 which shows the behavior of an element formed by a combination of  $90^\circ$  and  $180^\circ$  walls, two Bloch lines, and a crosstie inclusion. The  $180^\circ$  wall along the horizontal direction is bisected by a crosstie at roughly the midpoint. To interpret the image at remanence, recall that MFM is sensitive to the surface charges. The interiors of the domains have slowly varying magnetization and are thus weakly charged. The walls and the crossties, on the other hand, can be regarded as a dipole layer and the positive and negative charges appear in the MFM contrast. The bright-dark contrast near the walls and inclusion reflect charge distributions and from which we identify the direction of magnetization of the domains and boundary walls. The variation of the intensity in the interior of the domains is indicative of a nonconstant  $M$ , as indeed it should in the vicinity of Bloch line or a crosstie.

We now consider the magnetic behavior as an external field is applied along the hard axis. Like the previous elements, the familiar expansion and contraction of the domains is clearly visible. However, the position of the crosstie remains fixed albeit its size and intensity diminishes somewhat with the field. This convincingly shows that the crossties are pinned. The reduction in contrast as well as the tendency of the crossties to bend towards the right domain suggests the increasing attraction between the charges of the  $90^\circ$  wall and the crosstie as the distances between them are shortened through the growth of the right domain. The attraction displaces the charges at the crosstie and thus reduces the intensity. This process continues up to roughly  $70\ \text{Oe}$ , where the right domain has reached the crosstie and caused its annihilation. The length of the  $180^\circ$  wall appears to remain constant with increasing field, up to  $105\ \text{Oe}$  where the annihilation of the crosstie has occurred. Beyond this point, the evolution is similar to the four domain pattern except that the

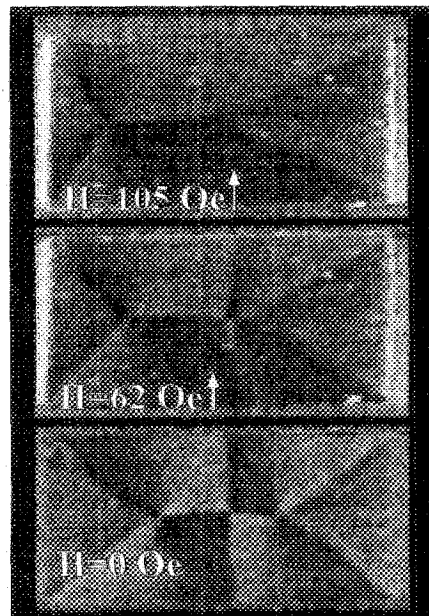


FIG. 4. Evolution of a  $2\ \mu\text{m} \times 4\ \mu\text{m}$  island with  $90^\circ$  and  $180^\circ$  walls, with Bloch lines and inclusion crosstie as a function of applied field along the hard axis. The charges and inferred magnetization for the zero field image is drawn in the bottom sketch.

complete collapse of the left pattern occurs well above the limit of our external field generator.

In conclusion, by using magnetic force microscopy, we have studied islands of different aspect ratios and shown some of the possible domain configurations and their evolutions in a field directed along the hard axis. The wall motion of a well-understood square element was initially studied to elucidate the interpretation of MFM images. The distinction between the MFM images of crossties and Bloch lines was clarified. In general, all islands showed reversible behavior at low fields, and irreversibility at high fields. Irreversible behavior is marked by the coalescence of two or more domains. The field required to produce irreversible behavior increased with aspect ratio, while crossties tend to pin domain wall movement.

This work was partially supported by the University of Maryland NSF MRSEC program. We appreciate the assistance of Dr. C. Krafft in manuscript preparation. Dr. Ed Burke lives in our hearts.

- <sup>1</sup>J. F. Smyth, S. Schultz, D. R. Fredkin, D. P. Kern, S. A. Rishton, H. Schmid, and M. Cali, *J. Appl. Phys.* **69**, 5262 (1991).
- <sup>2</sup>J.-G. Zhu, Y. Zheng, and X. Liu, *J. Appl. Phys.* **81**, 4336 (1997).
- <sup>3</sup>T. Schrefl, J. Fidler, K. J. Kirk, and J. N. Chapman, *J. Magn. Magn. Mater.* **175**, 193 (1997).
- <sup>4</sup>D. R. Fredkin, T. R. Koehler, J. F. Smyth, and S. Schultz, *J. Appl. Phys.* **69**, 5272 (1991).
- <sup>5</sup>S. J. Hefferman, J. N. Chapman, and S. McVitie, *J. Magn. Magn. Mater.* **95**, 76 (1991).
- <sup>6</sup>B. Khamsehpor, C. D. W. Wilkinson, J. N. Chapman, and A. B. Johnston, *J. Vac. Sci. Technol. B* **14**, 3361 (1996).
- <sup>7</sup>R. D. Gomez, I. D. Mayergoyz, and E. R. Burke, *IEEE Trans. Magn.* **31**, 3346 (1995).
- <sup>8</sup>R. D. Gomez, A. O. Pak, A. J. Anderson, E. R. Burke, A. J. Leyendecker, and I. D. Mayergoyz, *J. Appl. Phys.* **83**, 6226 (1998).
- <sup>9</sup>K. Runge, Y. Nozaki, Y. Otani, and H. Miyajima, *J. Appl. Phys.* **79**, 5075 (1996).